HHS Public Access

Author manuscript

Epilepsy Behav. Author manuscript; available in PMC 2019 November 01.

Published in final edited form as:

Epilepsy Behav. 2018 November ; 88: 87–95. doi:10.1016/j.yebeh.2018.06.038.

Temporal Lobe Epilepsy Affects Spatial Organization of Entorhinal Cortex Connectivity

Taylor Kuhn[a,c], **Joseph M. Gullett**[a,i], **Angelique E. Boutzoukas**[a], **Anastasia Bohsali**[e], **Thomas H. Mareci**[b], **David B. FitzGerald**[i], **Paul R. Carney**[d,e,f,g,h], and **Russell M. Bauer**[a,i]

[a]Department of Clinical and Health Psychology, University of Florida, Gainesville, FL, United States of America

[b]Department of Biochemistry and Molecular Biology, University of Florida, Gainesville, FL, United States of America

[c]Department of Physical Therapy, University of Florida, Gainesville, FL, United States of America

[d]Department of Pediatrics, University of Florida, Gainesville, FL, United States of America

[e]Department of Neurology, University of Florida, Gainesville, FL, United States of America

[f]Department of Neuroscience, University of Florida, Gainesville, FL, United States of America

[g]J. Crayton Pruitt Department of Biomedical Engineering, University of Florida, Gainesville, FL, United States of America

[h]B.J. and Eve Wilder Epilepsy Center Excellence, University of Florida, Gainesville, FL, United States of America

[i]Department of VA Brain Rehabilitation Research Center, Malcolm Randall VA Center Gainesville, FL, United States of America

Abstract

Evidence for structural connectivity patterns within the medial temporal lobe derives primarily from post-mortem histological studies. In humans and non-human primates, the parahippocampal gyrus (PHg) is subdivided into parahippocampal (PHc) and perirhinal (PRc) cortices which receive input from distinct cortical networks. Likewise, their efferent projections to the entorhinal cortex (ERc) are distinct. The PHc projects primarily to the medial ERc (M-ERc). The PRc projects primarily to the lateral portion of the ERc (L-ERc). Both M-ERc and L-ERc, via the perforant pathway, project to the dentate gyrus and hippocampal (HC) subfields. Until recently, these neural circuits could not be visualized *in vivo.* Diffusion tensor imaging algorithms have been developed to segment grey matter structures based on probabilistic connectivity patterns. However, these algorithms have not yet been applied to investigate connectivity in the temporal lobe or changes in connectivity architecture related to disease processes. In this study, this segmentation procedure

Corresponding Author: Taylor P Kuhn, Ph. D., Department of Clinical and Health Psychology, PO Box 100165, Gainesville, FL 32610; 321-698-1832 (phone). tkuhn@phhp.ufl.edu.

was used to classify ERc grey matter based on PRc, ERc, and HC connectivity patterns in 7 patients with temporal lobe epilepsy (TLE) without hippocampal sclerosis (mean age, 14.86 ± 3.34) and 7 healthy controls (mean age, 23.86 ± 2.97). Within samples paired t-tests allowed for comparison of ERc connectivity between epileptogenic and contralateral hemispheres. In healthy controls, there was no significant within-group differences in surface area, volume or cluster number of ERc connectivity-defined regions (CDR). Likewise, in line with histology results, ERc CDR in the control group were well organized, uniform and segregated via PRc/PHc afferent and HC efferent connections. Conversely, in TLE, there were significantly more PRc and HC CDR clusters in the epileptogenic than the contralateral hemisphere. The surface area of the PRc CDR were greater, and that of the HC CDRs was smaller, in the epileptogenic hemisphere as well. Further, there was no clear delineation between M-ERc and L-ERc connectivity with PRc, PHc or HC in TLE. These results suggest a breakdown of the spatial organization of PHg – ERc – HC connectivity in TLE. Whether this breakdown is the cause or result of epileptic activity remains an exciting research question.

INTRODUCTION

The medial temporal lobe (MTL) is a historically studied region which mediates numerous clinically significant cognitive functions including episodic memory. Different neuromedical illnesses, such as temporal lobe epilepsy (TLE), can affect the structure and function of the MTL. Therefore, understanding the unique effects of illness on the structure of MTL circuitry can provide insights into both the pathological process of the disease as well as the neuroanatomical basis of the clinical phenomenology of that disease. Relatedly, studying the effect of disease on the functional anatomy of memory circuits can provide additional insight into the mechanisms of MTL function.

Histological studies have illustrated the intra and interhemispheric connections of the medial temporal lobe circuits. The parahippocampal gyrus (PHg) can be subdivided along the rostrocaudal axis into the perirhinal cortex (PRc) and, more posteriorly, the parahippocampal cortex (PHc), with the dividing line roughly corresponding to the collateral sulcus[1]. This distinction is based on the existence of relatively distinct regions of input to the PRc/PHc. The PRc receives primary afferent input from the ventral visual stream[2]. In contrast, PHc input includes multimodal association cortices – parietal, supraoccipital, temporal auditory – as well as somesthetic cortex and the dorsal visual stream.

As the PHc and PRc receive separate streams of input, their efferent projections to the entorhinal cortex (ERc) are also distinct[1,3]. The PHc projects to the medial ERc (M-ERc) which projects to the dentate gyrus and hippocampal fields CA3 and CA1 via the perforant pathway[4]. Conversely, the PRc projects primarily to the lateral portion of the ERc (L-ERc). The L-ERc then sends afferent connections to different targets in the dentate gyrus, CA3, and CA1[5]. This pattern of connectivity creates two distinct temporal lobe circuits which may support behaviorally dissociable memory functions.

While postmortem histology studies have demonstrated the elegant complexities of these MTL memory circuits, our ability to visualize these circuits *in vivo* has been limited by image resolution and data analysis techniques. Structural neuroimaging studies have

successfully visualized large MTL white matter tracts and quantified them using diffusion metrics such as mean diffusivity (MD) and fractional anisotropy (FA)[6–12]. Functional neuroimaging studies have successfully delineated similar MTL circuits[13]. However, there has been limited research into structural connectivity patterns within the MTL. A probabilistic tractography method has been used to investigate patterns of connectivity between thalamic nuclei and cortex[14], striatal regions and cortex[15], amygdala nuclei and cortex[16] as well as amygdala nuclei and subcortical regions[17]. To the best of our knowledge, ours is the first attempt to use probabilistic tractography to visualize connectivity patterns involving the PRc, PHc, ERc and HC,

Temporal lobe epilepsy (TLE) is an excellent disease model for the study of MTL structure and function. In the last twenty years, quantitative structural MRI research within TLE patient populations has revealed volumetric reduction in temporal lobe structures including the temporal neocortex[18], the PHg[19], the ERc[20], and the fornix[21]. More recently, diffusion tensor imaging (DTI) studies have demonstrated white matter integrity changes in patients with TLE in white matter extending into the PHg, within the ipsilateral hippocampus[6], fornix[7, 9], into the inferior temporal gyrus and deep temporal white matter[9].

A promising DTI analytic tool, probabilistic tractography can be used to perform connectivity-based segmentation of grey matter structures[22]. Boundaries of anatomic structures cannot be easily identified *in vivo*, even with high resolution MRI. Use of differences in connectivity between adjacent and far structures can be used to identify anatomic boundaries in certain structures. Thus, differences in connectivity will allow structural boundaries to be defined, or segmented. This connectivity-based segmentation has not been used to investigate hippocampal or parahippocampal structures. Also absent has been using connectivity-based segmentation to examine the effect of TLE on white matter structures.

METHODS

This study was approved by the University of Florida Institutional Review Board as well as the North Florida/South Georgia Veterans Administration Hospital Institutional Review Board. All participants or their legal guardians provided written informed consent using forms approved by the University of Florida Institutional Review Board. In accordance with University of Florida Institutional Review Board. Seven individuals 10–26 years of age with physician-verified diagnosis of focal onset seizures of temporal lobe origin (TLE) were recruited from the University of Florida Comprehensive Epilepsy Program. Neuroimaging data from a group of seven age and gender matched healthy control individuals were procured from a collaborator's (DBF) study of white matter integrity. All participants were right handed from birth and native English speakers (Table 1). Participants with TLE had a clinical diagnosis of intractable, medically refractory (i.e. drug resistant) unprovoked focal onset epilepsy - affecting the temporal lobe - according to International League Against Epilepsy (ILAE) criteria for epilepsy diagnosis[23]. As part of a pre-surgical epilepsy evaluation, participants underwent continuous time-locked video-scalp EEG (phase 2) followed at a later date by continuous time-locked subdural temporal and extra-temporal frontal and parietal lobes electrocorticography (phase 2). All participants were candidates

for neurosurgical resection, however, none had undergone any neurosurgical intervention at the time of this study. Exclusionary criteria included diagnosis of neurodegenerative disorder, history of concussion or traumatic brain injury sufficient to warrant medical attention, previous psychiatric hospitalization, history of substance abuse, current psychotropic medication prescription (except anxiolytics and antidepressants), severe, uncorrected hearing or vision impairment and pregnancy. Additionally, epilepsy participants were excluded if structural neuroimaging (T1 or T2 data) revealed abnormalities by 3 T brain MR imaging and/or positron emission tomography (PET). MR imaging was negative for HS, dysplasia, malrotation and focal neoplasia in all participants. Further, two participants had a history of febrile status epilepticus (FSE) and were negative for herpes virus. Both patients underwent acute 3T MR imaging and follow-up 3T MR imaging was obtained approximately one year later. Visual interpretation by two neuroradiologists was supplemented by hippocampal volumetrics, analysis of the intrahippocampal distribution of T2 signal, and apparent diffusion coefficients. Hippocampal T2 hyperintensity occurred acutely after FSE in one participant in association with increased volume. The other patient showed a normal MR imaging acutely. Follow-up MR imaging obtained on both children was MR negative.

Imaging Protocol

Participants with TLE in this study underwent an MR imaging acquisition protocol currently employed in the University of Florida Comprehensive Epilepsy Center. For this protocol, T1-weighted structural data was used for manual segmentation of ROIs. T1-weighted, T2-weighted and FLAIR data were used to assess hippocampal sclerosis (used for secondary exclusion). 64-direction high angular direction diffusion imaging (HARDI), as well as 6-direction with three b0 images, were acquired for all participants.

T1-weighted and DWI data was collected using a 32-channel head coil on Siemens Magnetom 3T scanner (Siemens Medical Solution, Erlangen, Germany) at the University of Florida Shands Hospital Neuroimaging Center (Gainesville, Florida). Structural MP-RAGE T1-weighted scans were acquired with 120 – 1.0mm sagittal slices, FOV = 256mm (A-P) x 192 mm (FH), matrix = 256 – 192, TR = 450.0 ms, TE = 10.0 ms, Flip Angle = 8, voxel size = 1.0mm x 0.94 mm x 0.94 mm. Diffusion weighted images were acquired using single shot spin-echo planar imaging (EPI) with 60 × 2.0 mm axial slices (no gap), FOV = 256 mm (AP) x 256 mm (RL), matrix = 128 × 128, TR = 15200 ms, TE = 81 ms, Flip Angle = 30, b-value = 1000 s/mm^2, voxel size = 2.0 × 2.0 × 2.0 mm, and time of acquisition was 7 min 16 s.

Multimodal MRI data for all control participants was acquired using a Philips Achieva 3T scanner (Amsterdam, Netherlands) using a 32-channel SENSE head coil. Structural T1-weighted images were acquired with 130 – 1.0 mm sagittal slices, FOV = 240 mm (AP) – 180 mm (FH), matrix = 256 – 192, TR = 9.90 ms, TE = 4.60 ms, Flip Angle = 8, voxel size = 1.0 × 0.94 × 0.94 mm. Diffusion-weighted images were acquired using single shot spin-echo planar imaging (EPI) with 60 × 2.0mm axial slices (no gap), FOV = 224 mm (AP) x 224 mm (RL), matrix = 112 × 112, TR = 9509 ms, TE = 55 ms, Flip Angle = 90, b-value = 1000 s/mm^2, voxel size = 2.0 × 2.0 × 2.0 mm). All imaging data was pre-processed

uniformly in order to harmonize data streams across scanners. Data was processed using FSL software package version 6.0 (FMRIB software Library) (www.fmrib.ox.ac.uk.fsl)[24,25]. 6- and 64-direction DWI volumes were merged to create a single DWI data file for each participant in order to optimize the signal-to-noise ratio. This DWI data was eddy current corrected[25], skull stripped[26], and then diffusion tensors were fit to the data[27, 28].

Manual Segmentation of ROIs

Voxel size for both anatomical and diffusion-weighted scans was uniform across scanners. Therefore, segmentation protocols were carried out in an identical fashion for both age-matched control and TLE groups. Prior to segmenting experimental data, three independent raters (TK, JMG, AEB) received training on all manual segmentation protocols until an intra-rater reliability of ≥ 0.90 and an interrater spatial overlap reliability (Dice coefficient) of ≥ 0.80 for each region of interest (ROI) was achieved. Following this training, participant group classification was blinded from raters and each rater was assigned to segment one ROI in order to limit the effect of inter-rater variance on our results.

All manual segmentation was conducted using ITK-SNAP[29]. Published protocols were used to segment the PHc[30, 31], PRc[32, 33] and ERc[32, 33]. Conservative boundaries were used in order to clearly define the PHc as an ROI distinct from the PRc and ERc. The HC was automatically segmented using the FIRST model-based segmentation tool[34], part of the FSL software package FMRIB software Library. Each segmented mask was then "boundary corrected" to ensure that there is no overlap between any of the masks.

Each ROI was manually traced in each participant's native T1-weighted structural space. Skull stripped, T1-weighted whole brain data was registered to diffusion space using linear transform and tri-linear interpolation. All ROI masks were then registered to diffusion space using linear transformation and nearest neighbor interpolation and inspected for quality control. The four segmented ROIs and the resulting connectivity matrix are presented below.

Probabilistic Tractography

Probabilistic diffusion tractography was conducted using previously defined methods[22, 35] using 25,000 streamline samples per seed voxel to compute a connectivity distribution to each target mask. The manually segmented ERc mask was used as the seed mask. Manually segmented PRc, PHc and automatically segmented HC masks were used as target masks between which probability distributions of connectivity with the ERc seed mask were created. Rather than generating streamline fiber tracts between regions of interest (i.e. deterministic tractography), this method determines the probability that a voxel in the ERc is connected with each voxel in the target masks.

Probabilistic tractography was then used to segment ERc voxels into connectivity-defined regions (CDR) by classifying ERc seed voxels based on their highest connection probability to the target masks. The validity of this method has been previously demonstrated[36]. This method resulted in a color coded image of each participants' left and right ERc. Each ERc voxel was given the color of the target mask with which that voxel has the highest probability of connecting, defined as the largest number of streamline samples between that

ERc voxel and a target mask. All ERc voxels assigned to a specific target mask compose a connectivity defined region (CDR) (e.g. with the HC) of the ERc (Figure 1).

Using FSL software, surface area was computed for each CDR of the hard segmented ERc for subsequent groupwise analyses. These values were then converted to proportion of the total ERc surface area in order to yield relative proportion of the entire ERc connecting to each target mask. In order to minimize the scanner-by-group confound, within-group paired sample t-tests were conducted to assess differences in proportional ERc CDR surface area between epileptogenic and contralateral hemispheres. Additionally, the number of CDR clusters was computed for each ERc. One cluster indicated that a CDR was contiguous. More than one cluster indicated that a CDR was not contiguous. Rather, the CDR was split into multiple smaller, less organized clusters. This was based on the hypothesis that in normal ERc tissue CDR are contiguous, there should be only one cluster per CDR. Therefore, additional clusters may represent alterations in spatial connectivity.

The TLE group was comprised of four participants with epileptogenic foci in the left hemisphere and three participants with epileptogenic foci in the right hemisphere. Paired samples t-tests were conducted to assess differences in the number of CDR clusters between the epileptogenic and contralateral hemispheres within the TLE group. Paired samples t-tests also compared the number of CDR clusters in controls after randomly choosing three control participants and flipping the hemispheric orientation of their data so that it mirrored that of the TLE group (four left and three right hemisphere).

RESULTS

ERc CDR across control participants were highly organized such that voxels comprising CDR were contiguous and well separated from other CDR (i.e. voxels were not intermingled). In accordance with histology results, the medial portion of the ERc connected to the PHc, the lateral portion connected to the PRc and, primarily in posterior slices, the central portion of the ERc connected to the HC (Figure 2).

Analysis of qualitative results revealed that there were between-group differences in the spatial organization of ERc CDR. Unlike those in the control group, the ERc CDR across participants with TLE diagnoses showed high degrees of variability in spatial organization (Figure 3). Voxels comprising CDR were less segregated, often displaying tessellated patterns of CDR voxels intertwining between one another (e.g. HC CDR voxels interspersed throughout PHc and PRc CDR voxels; Figure 3). Additionally, the spatial organization of ERc CDR in the TLE group did not reflect the histologically-derived connectivity pattern. PHc and PRc connections were not restricted to the medial and lateral portion of the ERc, respectively, and HC connections appeared to be randomly distributed throughout the ERc.

Paired samples t-tests revealed significant differences in the number of CDR clusters in the epileptogenic hemisphere compared to the contralateral hemisphere in the TLE group. In the epileptogenic hemisphere, there were significantly more PRc CDR clusters ($t(6)= 3.29$, $p = 0.017$) and HC CDR clusters ($t(6)= 3.87$, $p = 0.008$) than in the contralateral hemisphere. The number of PHc clusters did not significantly differ between epileptogenic and

contralateral hemisphere. There were no significant interhemispheric differences in the number of clusters within the control group (all p's > 0.05) (Table 2).

Additionally, paired samples t-tests revealed significant interhemispheric differences in the surface area of CDR in the TLE group. The surface area of the PRc CDR was significantly larger in the epileptogenic hemisphere ($t(6)= 2.18$, $p = 0.048$) and the HC CDR was significantly smaller in the epileptogenic hemisphere ($t(6)= -2.16$, $p = 0.050$). There were no significant interhemispheric differences in CDR surface area in the control group (all p's > 0.05) (Table 3).

DISCUSSION

This study represents the first successful *in vivo* visualization of two adjacent PHg – ERc – HC circuits as applied to a clinical population[36]. Through the use of probabilistic tractography and connectivity-based segmentation, we were able to successfully demonstrate the existence of separate, adjacent medial temporal lobe circuits. A uniform organization of bilateral ERc was observed in control participants consistent with histological findings in excised human tissue. The structure of CDR of the ERc shows the PRc projecting to the lateral ERc and the PHc projecting to the medial ERc. These two efferent streams appear to join towards the center of the ERc and become afferent projections to the HC.

In contrast, the TLE group white matter organization was less spatially defined. The CDR's were less well segregated and there were more clusters between CDRs in the TLE patients. Projections from the PHc and PRc and to the HC were spread more diffusely throughout the ERc and were not restricted to medial/lateral portions of the ERc, as they were in the control group. Further, in the control group, bilateral PRc, left PHc and HC ERc CDR and the majority of right PHc and HC were contiguous throughout the ERc, as indicated by one CDR cluster. Alternatively, no CDR was contiguous throughout the entirety of the ERc in any participant with TLE. With the exception of the right HC CDR, each CDR in the TLE group was less unified, as indicated by two or more clusters. Further, in the TLE group, there were more PRc and HC CDR clusters within the epileptogenic hemisphere than the contralateral hemisphere. Interestingly, the surface area of the PRc CDR was greater in the epileptogenic hemisphere while the surface area of the HC CDR was greater in the contralateral hemisphere. While we can only postulate about this finding, it is possible that this greater surface area in the epileptogenic hemisphere is indicative of less pruning leading to less organized (i.e. more clusters) structures with increased likelihood for producing seizures. Taken together, this demonstrates a loss of spatial organization in these medial temporal lobe circuits characterized by reduced spatial specificity of white matter connections (i.e. increased CDR clusters) and alterations in the degree of connectivity between regions. More random topological organization of neural networks has been shown to increase an individual's susceptibility to seizure[37]. This can lead to a feed-forward cycle of seizures causing structural brain changes which reduce the threshold for future ictal onset (i.e. kindling). Thus, enhanced connectivity of the PRc – ERc – HC circuit may be the result of seizure related remodeling of structural neural networks. Additionally, the decreased surface area of the HC CDR in the epileptogenic hemisphere could be related to this aberrant remodeling and may be involved in TLE-associated memory deficits.

Although our findings cannot confirm that structural changes preceded, as has been previously suggested[38], or were the result of epileptogenic activity, it is conceivable that seizure activity resulted in the loss of spatial organization in ERc CDR. Following repetitive seizures of multiple etiologies, structural changes and reorganization occur in the temporal lobe including loss of mossy cells and hilar interneurons[39–41]. This degeneration is followed by mossy fiber sprouting resulting in the formation of recurrent collaterals between granule cells[39,41]. In the healthy brain, granule cells do not form synapses with other granule cells. In the epileptic brain, these aberrant granule cell to granule cell synapses are excitatory in nature and in the postictal stage often produce an increased number of outgoing connections[42]. This enhanced connectivity within the dentate gyrus results in a novel neural hub shown to provide a mechanism for promoting hyperexcitability leading to recurrent seizures[43].

All participants with TLE in this study were MR-negative for hippocampal sclerosis (HS), dysplasia, and focal neoplasia, all of which are the common structural abnormalities in individuals with drug-resistant TLE. MTL pathology in TLE is often verified with high reliability using MR imaging and is believed to reflect a combination of initial damage from an early injury and subsequent seizure-associated injury.[44–47] However, as with our study, no pathological MR imaging findings in individuals with TLE are reported in up to one-third of patients[48,49]. It remains a controversy whether this is due to initial disease stages which do not display lesional findings in MR imaging because of subtle tissue alterations or based on different illness-entities affecting hippocampal structures. Similarly, two of the TLE participants (29%) had a history of febrile seizures: one with T2 hyperintense and hippocampal volume hypertrophy at baseline which resolve at one-year follow-up (MR imaging negative at that time); one with normal MR imaging findings at both time points. Given this, it could be speculated that the greater number of CDRs found in the epileptogenic MTL regions resulted from seizure activity, rather than from an aberrant neurodevelopmental trajectory leading to seizure formation. However, given that this was not a longitudinal study, and fine grained DTI analysis was not performed prior to seizure onset in these participants, this question remains unanswered. Nevertheless, given that all participants were MR-negative for cortical dysplasias, it is unlikely that increased PRc CDR number and surface area reflect occult cortical dysplasia. Rather, it is possible that these PRc CDR findings are related to axonal reorganization related to seizure activity (discussed further below).

These findings are in line with recent investigations of regional network characteristics in TLE, which have broadly demonstrated abnormalities in network topologies related to epileptogenicity. Previous structural network analyses reported decreased structural organization between MTL and limbic regions[50–52], thalamic and neocortical regions[53,54], and within cortico-cortical networks[52,55]. Additionally, reduced cortical-subcortical connectivity, most prominent in the MTL but occurring throughout the brain, have been observed in unilateral TLE[56]. Importantly, these structural connectivity analyses were restricted to large scale connections between MTL regions (e.g. hippocampus, amygdala) and other more distal brain regions (e.g. limbic, frontal and basal ganglia areas). Therefore, our findings appear to be, to the best of our knowledge, one of the first studies to replicate

these aberrant structural connectivity results within highly proximal MTL regions within the epileptogenic zone.

Further, our findings fit within the context of the literature on TLE-related reorganization of structural connectivity network. An atrophic consequence of repeated epileptogenic propagation throughout the MTL network[57] may be related to the reduced spatial organization and smaller CDR found in the present study. Therefore, it is possible that the (likely Hebbian-in-nature) enhanced connectivity of the PRc – ERc – HC circuit increases the probability of subsequent seizures and that those subsequent seizures simultaneously result in atrophic and/or aberrantly plastic reorganization of the PHc-ERc_HC circuit. This hypothesis is supported by TLE-related structural reorganization of the hippocampus and limbic system[58,59], which may include increased local fragmentation within the limbic system[58] along with decreased hippocampal cliquiness (or segregation as evidenced by clustering coefficient) and increased though poorly organized hippocampal connectivity (i.e. nodal degree)[58]. Taken together, these findings suggest decreased structural segregation of the hippocampus from surrounding networks due to loss of local white matter connectivity and increased, non-local projections which ultimately result in an overall reduction in local efficiency[53]. Such aberrant connectivity, likely formed via dentate hilar cell loss[60] may lead to the higher connectivity between local MTL structures leading to kindling and subsequent increased epileptogenic activity.

Regardless of exact etiology, alterations in structural connectivity in TLE deleteriously impact functional connectivity networks, including changes in local and global efficiency and covariance[61–63]. For example, reduced functional network integration of the hippocampus in TLE has been associated with seizure-induced atrophy while parahippocampal connectivity was effected by coherence of white matter tracts subserving this functional connectivity[64]. Although not directly analogous, our PHg connecitivity findings may relat to these TLE-related coherence abnormalities. Further, a graph theory study[65] found increased covariance within-MTL regions, possibly indicative of axonal sprouting, and decreased coherence between regions, possibly reflecting loss of connectivity between structures. Similarly, decreased functional connectivity between regions of the epileptogenic TLE, without any significant findings of within region connectivity abnormalities have been reported[66]. Likely due to the fact that increased distal connectivity is often indicative of a mechanism attempting to compensate for reduced functional connectivity between more local regions[67–69], such as those connectivity abnormalities reported herein, hippocampal connectivity to regions outside the focal epileptogenic MTL (e.g. limbic cortex, frontal, basal ganglia and brainstem regions as well as default mode, sensory and motor networks) has been reported[70]. Our findings of decreased spatial organization of CDR as well as the decreased surface area of PHc CDR may relate to these decreased coherence findings. Overall, our findings add to the literature of structural and functional connectomics of TLE and further support the necessity of ongoing translational research in this field[71].

Importantly, our TLE patient group was significantly younger than our control group. Therefore, the impact of neurodevelopment on structural organization and connectivity may be more prominent in the TLE group than in the somewhat older control group. Our

participants were experiencing seizures over a prolonged period of time during development. The prolonged nature of seizures during critical neurodevelopmental periods may have allowed transient, peri-ictal changes in neural connectivity to become chronic. Additionally, seizure activity along with predisposing genetic risk factors, which may have been present in some of our participants, could have resulted in disorganized white matter connectivity in these adjacent temporal lobe circuits. Given the average age of our participants, and the fact that pruning tends to end at approximately 16 years of age[72], it could be argued that our findings reflect connectivity patterns indicative, not of epileptogenic activity, but of brains which have not yet completed the process of pruning. However, this is unlikely given that our participants ranged in age from 10–26 and the loss of spatial organization in ERc connectivity was found in all TLE participants.

Additionally, earlier age of seizure onset may disrupt neural development and lead to cerebral reorganization, often with measurable negative consequences on specific domains of cognitive function. Higher rates of bilateral and right hemisphere language dominance are seen among patients with TLE[73]. Abnormal organization of language[74,75] and memory[76] have been demonstrated in early onset TLE patients. Therefore, it is possible that the aberrant connectivity found in our younger TLE group was related to, and perhaps the result of, recurrent epileptic activity rather than normal neurodevelopmental differences inherent in late adolescence. Additionally, studies suggest that gender affects morphology more than age, at the level of cortical sulci[77]. Given that cortical morphometry dictated manual segmentation procedures, future studies may seek to investigate the effect of gender on spatial organization.

This study had several limitations. First, group was confounded with scanner platform; control data was acquired using a 3T Philips Achieva, while patients with TLE underwent MRI using a Siemens Magnetom 3T scanner. However, this confound was overcome by harmonizing MR data processing and then focusing our analyses on within group, paired samples tests. By doing so, the effect of scanner platform was removed from our analyses. Further, the ability to produce reliable CDR from small medial temporal lobe regions using manual segmentation of 64-direction HARDI data, as done in this study, has been shown[36]. Nevertheless, limitations inherent in probabilistic tractography include hypersensitivity to non-dominant fiber pathway orientation and proneness to false positive errors, both of which may limit the precision with which it reproduces neuroanatomy. Additionally, spatial resolution is limited to the scale of MR imaging resolution resulting in an inability to differentiate afferent from efferent connections or detect neuronal polarity or synapses. Although some of these limitations are lessened by HARDI acquisition and evidence-based processing pipeline approaches such as that used here, some remain (e.g. that diffusion imaging is an indirect measure of neuronal architecture and thus cannot make direct inferences about effects at the cellular level) and must be taken into consideration when interpreting results. Further, attempting to reproduce our results using automatic segmentation protocols (e.g. using Freesurfer to parcellate the hippocampus into subfields) may allow for more fine grained spatial analysis.

Additionally, even for neuroimaging studies our sample size was small. Replication of our analysis in a larger independent sample is warranted. A greater sample size would also

provide additional variance and degrees of freedom in our statistical analyses which could be used to further investigate the relationship between seizure duration, seizure frequency and integrity/connectivity of structures within the medial temporal lobe.

Despite these limitations, the study represents a meaningful contribution to the literature on TLE and the functional neuroanatomy of memory and supports the hypothesis that TLE is associated with pathologic changes in white matter connectivity in MTL regions. Future studies may use the tractography-based CDR method used here to map the developmental trajectory of MTL connectivity and investigate the effect of neuromedical illness on the structure and function of this region. Longitudinal studies, particularly large cohort studies which begin in infancy and follow participants to see who develops epilepsy and what neuroanatomical markers predicted conversion to epilepsy, can help elucidate whether finding such as ours predate and possibly contribute to the development of seizures or represent aberrant changes brought about after the onset of seizures.

Funding/Support/Acknowledgements

This research was supported by grant funding from the Department of Veterans Affairs RR&D Diffusion Tensor Imaging of White Matter After Traumatic Injury CDA-2 # B6698W (DBF); the State of Florida Brain and Spinal Cord Injury Research Trust Fund (BSCRITF) Correlating Disturbed Sleep and Damaged White Matter Tracts in the Brainstem in Traumatic Brain Injury Using Diffusion Weighted Imaging (DBF,THM); USAMRMC/TATRC-Correlating Sleep Disturbances and Damaged White Matter Tracts in the Brainstem using Diffusion Weighted Imaging (Contract #W81XH-11–1-0454) (DBF,THM); National Institutes of Grant R01 NS082522 (PRC); National Institutes of Grant RO1NS077004 (PRC); National Institutes of Grant R01 NS082522 (PRC); National Institutes of Grant R21 NS081646 (PRC); and the B.J. and Eve Wilder Center of Excellence for Epilepsy Research (AEB, PRC). The contents of this paper do not represent the views of the U.S. Department of Veterans Affairs, Department of Defense or the United States Government. The authors report no conflicts of interest.

REFERENCES

1. Eichenbaum H, Yonelinas AP, & Ranganath C (2007). The medial temporal lobe and recognition memory. Annu Rev Neurosci, 30, 123–152. [PubMed: 17417939]
2. Holdstock JS, Hocking J, Notley P, Devlin JT, & Price CJ (2009). Integrating visual and tactile information in the perirhinal cortex. Cerebral Cortex, 19, 2993–3000. [PubMed: 19386635]
3. Diana RA, Yonelinas AP, & Ranganath C (2007). Imaging recollection and familiarity in the medial temporal lobe: a three-component model. Trends Cogn Sci, 11(9), 379–386. [PubMed: 17707683]
4. Kerr KM, Agster KL, Furtak SC, & Burwell RD (2007). Functional neuroanatomy of the parahippocampal region: the lateral and medial entorhinal areas. Hippocampus, 17(9), 697–708. [PubMed: 17607757]
5. Furtak SC, Wei SM, Agster KL, & Burwell RD (2007). Functional neuroanatomy of the parahippocampal region in the rat: the perirhinal and postrhinal cortices. Hippocampus, 17(9), 709–722. [PubMed: 17604355]
6. Salmenpera TM, Simister RJ, Bartlett P, Symms MR, Boulby PA, Free SL,…Duncan JS (2006). High-resolution diffusion tensor imaging of the hippocampus in temporal lobe epilepsy. Epilepsy Res, 71(2–3), 102–106. [PubMed: 16870399]
7. Concha L, Beaulieu C, & Gross DW (2005). Bilateral limbic diffusion abnormalities in unilateral temporal lobe epilepsy. Ann Neurol, 57(2), 188–196. [PubMed: 15562425]
8. Concha L, Beaulieu C, Collins DL, & Gross DW (2009). Whitematter diffusion abnormalities in temporal-lobe epilepsy with and without mesial temporal sclerosis. Journal of Neurology, Neurosurgery & Psychiatry, 80(3), 312–319.
9. Focke NK, Yogarajah M, Bonelli SB, Bartlett PA, Symms MR, & Duncan JS (2008). Voxel-based diffusion tensor imaging in patients with mesial temporal lobe epilepsy and hippocampal sclerosis. Neuroimage, 40(2), 728–737. [PubMed: 18261930]

10. Lin JJ, Riley JD, Juranek J, & Cramer SC (2008). Vulnerability of the frontal-temporal connections in temporal lobe epilepsy. Epilepsy Res, 82(2–3), 162–170. [PubMed: 18829258]
11. Matsumoto R, Okada T, Mikuni N, Mitsueda-Ono T, Taki J, Sawamoto N, et al. (2008). Hemispheric asymmetry of the arcuate fasciculus: a preliminary diffusion tensor tractography study in patients with unilateral language dominance defined by Wada test. J Neurol, 255(11), 1703–1711. [PubMed: 18821045]
12. Ahmadi ME, Hagler DJ, Jr., McDonald CR, Tecoma ES, Iragui VJ, Dale AM, et al. (2009). Side matters: diffusion tensor imaging tractography in left and right temporal lobe epilepsy. AJNR Am J Neuroradiol, 30(9), 1740–1747. [PubMed: 19509072]
13. Kahn I, Andrews-Hanna JR, Vincent JL, Snyder AZ, & Buckner RL (2008). Distinct cortical anatomy linked to subregions of the medial temporal lobe revealed by intrinsic functional connectivity. Journal of neurophysiology, 100(1), 129–139. [PubMed: 18385483]
14. Johansen-Berg H, Behrens EJ, Sillery E, Ciccarelli O, Thompson AJ, Smith SM, & Matthews PM (2004). Functional-Anatomical Validation and Individual Variation of Diffusion Tractography-based Segmentation of Human Thalamus. Cerebral Cortex, 15, 31–39. [PubMed: 15238447]
15. Tziortzi AC, Haber SN, Searle GE, Tsoumpas C, Long CJ, Shotbolt P, & Gunn RN (2014). Connectivity-based functional analysis of dopamine release in the striatum using diffusion-weighted MRI and positron emission tomography. Cerebral Cortex, 24(5), 1165–1177. [PubMed: 23283687]
16. Bach DR, Behrens TE, Garrido L, Weiskopf N, & Dolan RJ (2011). Deep and superficial amygdala nuclei projections revealed in vivo by probabilistic tractography. The Journal of Neuroscience, 31(2), 618–623. [PubMed: 21228170]
17. Saygin ZM, Osher DE, Augustinack J, Fischl B, & Gabrieli JD (2011). Connectivity-based segmentation of human amygdala nuclei using probabilistic tractography. Neuroimage, 56(3), 1353–1361. [PubMed: 21396459]
18. Lencz T, McCarthy G, Bronen RA, Scott TM, Inserni JA, Sass KJ,& Spencer DD (1992). Quantitative magnetic resonance imaging in temporal lobe epilepsy: relationship to neuropathology and neuropsychological function. Ann Neurol, 31(6), 629–637. [PubMed: 1514774]
19. Bernasconi N, Natsume J, & Bernasconi A. (2005) Progression in temporal lobe epilepsy: differential atrophy in mesial temporal structures. Neurology 65:223–228. [PubMed: 16043790]
20. Bernasconi N, Bernasconi A, Andermann F, Dubeau F, Feindel W, & Reutens DC (1999). Entorhinal cortex in temporal lobe epilepsy: a quantitative MRI study. Neurology, 52(9), 1870–1876. [PubMed: 10371536]
21. Kuzniecky R, Bilir E, Gilliam F, Faught E, Martin R, & Hugg J (1999). Quantitative MRI in temporal lobe epilepsy: evidence for fornix atrophy. Neurology, 53(3), 496–501. [PubMed: 10449110]
22. Behrens TEJ, Johansen-Berg H, Woolrich MW, Smith SM, Wheeler-Kingshott CA, Boulby PA,… & Matthews PM (2003a) Non-invasive mapping of connections between human thalamus and cortex using diffusion imaging. Nat Neurosci 6:750–757. [PubMed: 12808459]
23. Fisher RS, Cross JH, French JA, Higurashi N, Hirsch E, Jansen FE,… & Scheffer IE (2017). Operational classification of seizure types by the International League Against Epilepsy: Position Paper of the ILAE Commission for Classification and Terminology. Epilepsia, 58(4), 522–530. [PubMed: 28276060]
24. Jenkinson M & Smith SM (2001). A global optimisation method for robust affine registration of brain images. Medical Image Analysis, 5(2):143–156 [PubMed: 11516708]
25. Smith SM (2002b). Fast robust automated brain extraction. Human Brain Mapping, 17(3):143–155. [PubMed: 12391568]
26. Smith SM, Zhang Y, Jenkinson M, Chen J, Matthews PM, Federico A & De Stefano N (2002). Accurate, robust and automated longitudinal and cross-sectional brain change analysis. NeuroImage, 17(1):479–489. [PubMed: 12482100]
27. Basser PJ, Mattiello J, & LeBihan D (1994). Estimation of the effective self-diffusion tensor from the NMR spin echo. J Magn Reson B;103:247–254. [PubMed: 8019776]

28. Pierpaoli C, Jezzard P, Basser PJ, Barnett A, & Di Chiro G (1996). Diffusion Tensory MR Imaging of the Human Brain. Radiology 201, 637–648. [PubMed: 8939209]
29. Yushkevich PA, Piven J, Hazlett HC, Smith RG, Ho S, Gee JC, & Gerig G (2006). User-guided 3D active contour segmentation of anatomical structures: significantly improved efficiency and reliability. Neuroimage, 31(3), 1116–1128. [PubMed: 16545965]
30. Rogalski EJ, Murphy CM, deToledo-Morrell L, Shah RC, Moseley ME, Bammer R, & Stebbins GT (2009). Changes in parahippocampal white matter integrity in amnestic mild cognitive impairment: a diffusion tensor imaging study. Behavioural neurology, 21(1), 51–61. [PubMed: 19847045]
31. Burgmans S, Van Boxtel MPJ, Smeets F, Vuurman EFPM, Gronenschild EHBM, Verhey FRJ, & Jolles J (2009). Prefrontal cortex atrophy predicts dementia over a six-year period. Neurobiology of aging, 30(9), 1413–1419. [PubMed: 18258339]
32. Insausti R, Juottonen K, Soininen H, Insausti AM, Partanen K, Vainio P & Pitkänen A (1998). MR volumetric analysis of the human entorhinal, perirhinal, and temporopolar cortices. American Journal of Neuroradiology, 19(4), 659–671. [PubMed: 9576651]
33. Franckó E, Insausti AM, Artacho-Pérula E, Insausti R, & Chavoix C (2012). Identification of the human medial temporal lobe regions on magnetic resonance images. Human Brain Mapping, doi: 10.1002/hbm.22170. [Epub ahead of print]; PMID: . [PubMed: 22936605]
34. Patenaude B, Smith SM, Kennedy D, & Jenkinson M (2011). A Bayesian Model of Shape and Appearance for Subcortical Brain. NeuroImage, 56(3), 907–922. [PubMed: 21352927]
35. Behrens TEJ, Woolrich MW, Jenkinson M, Johansen-Berg H, Nunes RG, Clare S,… & Smith SM (2003b) Characterization and propagation of uncertainty in diffusion-weighted MR imaging. Magn Reson Med 50:1077–1088. [PubMed: 14587019]
36. Kuhn T, Gullett JM, Boutzoukas AE, Ford A, Nguyen P, Colon-Perez LM, Triplett W, …& Bauer RM (2015). Test-Retest Reliability of High Angular Resolution Diffusion Imaging (HARDI) Acquisition Assessed via TBSS, Tractography and a Novel Graph Theory Metric. Brain Imaging and Behavior.
37. Douw L, van Dellen E, de Groot M, Heimans JJ, Klein M, Stam CJ, & Reijneveld JC (2010). Epilepsy is related to theta band brain connectivity and network topology in brain tumor patients. BMC neuroscience, 11(1), 103. [PubMed: 20731854]
38. Liu RS, Lemieux L, Bell GS, Sisodiya SM, Bartlett PA, Shorvon SD,… & Duncan JS (2002). The structural consequences of newly diagnosed seizures. Annals of neurology, 52(5), 573–580. [PubMed: 12402254]
39. Buckmaster PS, & Jongen-Rêlo AL (1999). Highly specific neuron loss preserves lateral inhibitory circuits in the dentate gyrus of kainite-induced epileptic rats. Journal of Neuroscience, 19(21), 9519–9529. [PubMed: 10531454]
40. Santhakumar V, Aradi I, & Soltesz I (2005). Role of mossy fiber sprouting and mossy cell loss in hyperexcitability: a network model of the dentate gyrus incorporating cell types and axonal topography. Journal of neurophysiology, 93(1), 437–453. [PubMed: 15342722]
41. Dyhrfjeld-Johnsen J, Santhakumar V, Morgan RJ, Huerta R, Tsimring L, & Soltesz I (2007). Topological determinants of epileptogenesis in large-scale structural and functional models of the dentate gyrus derived from experimental data. Journal of neurophysiology, 97(2), 1566–1587. [PubMed: 17093119]
42. Walter C, Murphy BL, Pun RY, Spieles-Engemann AL, & Danzer SC (2007). Pilocarpine-induced seizures cause selective timedependent changes to adult-generated hippocampal dentate granule cells. Journal of Neuroscience, 27(28), 7541–7552. [PubMed: 17626215]
43. Howard AL, Neu A, Morgan RJ, Echegoyen JC, & Soltesz I (2007). Opposing modifications in intrinsic currents and synaptic inputs in post-traumatic mossy cells: evidence for single-cell homeostasis in a hyperexcitable network. Journal of Neurophysiology, 97(3), 2394–2409. [PubMed: 16943315]
44. Duc CO, Trabesinger AH, Weber OM, Meier D, Walder M, Wieser HG, & Boesiger P (1998). Quantitative 1H MRS in the evaluation of mesial temporal lobe epilepsy in vivo. Magnetic resonance imaging, 16(8), 969–979. [PubMed: 9814780]

45. Lee DH, Gao FQ, Rogers JM, Gulka I, Mackenzie IR, Parrent AG,… & Girvin JP (1998). MR in temporal lobe epilepsy: analysis with pathologic confirmation. American Journal of Neuroradiology, 19(1), 19–27. [PubMed: 9432153]
46. Park SW, Chang KH, Kim HD, Song IC, Lee DS, Lee SK,… & Park YH (2001). Lateralizing ability of single-voxel proton MR spectroscopy in hippocampal sclerosis: comparison with MR imaging and positron emission tomography. American journal of neuroradiology, 22(4), 625–631. [PubMed: 11290468]
47. Wellard RM, Briellmann RS, Prichard JW, Syngeniotis A, & Jackson GD (2003). Myoinositol abnormalities in temporal lobe epilepsy. Epilepsia, 44(6), 815–821. [PubMed: 12790895]
48. Van Paesschen W, Connelly A, Johnson CL, & Duncan JS (1996). The amygdala and intractable temporal lobe epilepsy A quantitative magnetic resonance imaging study. Neurology, 47(4), 1021–1031. [PubMed: 8857739]
49. Hammen T, Kerling F, Schwarz M, Stadlbauer A, Ganslandt O, Keck B,… & Stefan H (2006). Identifying the affected hemisphere by 1Hwww.w3.org/1999/xlinkMR spectroscopy in patients with temporal lobe epilepsy and no pathological findings in high resolution MRI. European journal of neurology, 13(5), 482–490.
50. Bonilha L, Rorden C, Halford JJ, Eckert M, Appenzeller S, Cendes F, & Li LM (2007). Asymmetrical extra-hippocampal grey matter loss related to hippocampal atrophy in patients with medial temporal lobe epilepsy. *Journal of* Neurology, Neurosurgery & Psychiatry, 78(3), 286–294.
51. Bernhardt BC, Worsley KJ, Besson P, Concha L, Lerch JP, Evans AC, et al. (2008). Mapping limbic network organization in temporal lobe epilepsy using morphometric correlations: insights on the relation between mesiotemporal connectivity and cortical atrophy. Neuroimage 42, 515–524. doi: 10.1016/j.neuroimage.2008.04.261 [PubMed: 18554926]
52. Mueller SG, Laxer KD, Barakos J, Ian C, Garcia P, and Weiner MW (2009a). Widespread neocortical abnormalities in temporal lobe epilepsy with and without mesial sclerosis. Neuroimage 46, 353–359. doi: 10.1016/j.neuroimage.2009.02.020 [PubMed: 19249372]
53. Mueller SG, Laxer KD, Barakos J, Cheong I, Finlay D, Garcia P, et al. (2009b). Involvement of the thalamocortical network in TLE with and without mesiotemporal sclerosis. Epilepsia. doi: 10.1111/j.1528-1167.2009.02413.x
54. Bernhardt BC, Bernasconi N, Kim H, and Bernasconi A (2012). Mapping thalamocortical network pathology in temporal lobe epilepsy. Neurology 78, 129–136. doi: 10.1212/WNL.0b013e31823efd0d [PubMed: 22205759]
55. Bernhardt B, Hong SJ, Bernasconi A, & Bernasconi N (2013). Imaging structural and functional brain networks in temporal lobe epilepsy. Frontiers in human neuroscience, 7, 624. [PubMed: 24098281]
56. Yasuda CL, Chen Z, Beltramini GC, Coan AC, Morita ME, Kubota B,… & Gross DW (2015). Aberrant topological patterns of brain structural network in temporal lobe epilepsy. Epilepsia, 56(12), 1992–2002. [PubMed: 26530395]
57. Abdelnour F, Mueller S, & Raj A (2015). Relating cortical atrophy in temporal lobe epilepsy with graph diffusion-based network models. PLoS computational biology, 11(10), e1004564. [PubMed: 26513579]
58. Bonilha L, Nesland T, Martz GU, Joseph JE, Spampinato MV, Edwards JC, et al. Medial temporal lobe epilepsy is associated with neuronal fibre loss and paradoxical increase in structural connectivity of limbic structures. J Neurol Neurosurg Psychiatry 2012;83:903–9. [PubMed: 22764263]
59. Chiang S, & Haneef Z (2014). Graph theory findings in the pathophysiology of temporal lobe epilepsy. Clinical Neurophysiology, 125(7), 1295–1305. [PubMed: 24831083]
60. Margerison J, Corsellis J. (1966). Epilepsy and the temporal lobes: A clinical electroencephalographic and neuropatholoical study of the brain in epilepsy, with particular reference to the temporal lobes. Brain;89:499–530. [PubMed: 5922048]
61. Bernhardt BC, Chen Z, He Y, Evans AC, & Bernasconi N (2011). Graph-theoretical analysis reveals disrupted small-world organization of cortical thickness correlation networks in temporal lobe epilepsy. Cerebral cortex, 21(9), 2147–2157. [PubMed: 21330467]

62. Vaessen MJ, Jansen JF, Vlooswijk MC, Hofman PA, Majoie HM, Aldenkamp AP, & Backes WH (2011). White matter network abnormalities are associated with cognitive decline in chronic epilepsy. Cerebral cortex, 22(9), 2139–2147. [PubMed: 22038907]

63. Liu M, Chen Z, Beaulieu C, & Gross DW (2014). Disrupted anatomic white matter network in left mesial temporal lobe epilepsy. Epilepsia, 55(5), 674–682. [PubMed: 24650167]

64. Voets NL, Beckmann CF, Cole DM, Hong S, Bernasconi A, & Bernasconi N (2012). Structural substrates for resting network disruption in temporal lobe epilepsy. Brain, 135(8), 2350–2357. [PubMed: 22669081]

65. Bernhardt BC, Bernasconi N, Hong SJ, Dery S, & Bernasconi A (2015). Subregional mesiotemporal network topology is altered in temporal lobe epilepsy. Cerebral cortex, 26(7), 3237–3248. [PubMed: 26223262]

66. Besson P, Bandt SK, Proix T, Lagarde S, Jirsa VK, Ranjeva JP,… & Guye M (2017). Anatomic consistencies across epilepsies: a stereotactic-EEG informed high-resolution structural connectivity study. Brain, 140(10), 2639–2652. [PubMed: 28969369]

67. Haneef Z, Lenartowicz A, Yeh HJ, Engel J, & Stern JM (2012). Effect of lateralized temporal lobe epilepsy on the default mode network. Epilepsy & Behavior, 25(3), 350–357. [PubMed: 23103309]

68. Zhang Z, Lu G, Zhong Y, Tan Q, Liao W, Wang Z,… & Liu Y (2010). Altered spontaneous neuronal activity of the default-mode network in mesial temporal lobe epilepsy. Brain research, 1323, 152–160. [PubMed: 20132802]

69. Mankinen K, Jalovaara P, Paakki JJ, Harila M, Rytky S, Tervonen O,… & Kiviniemi V (2012). Connectivity disruptions in resting-state functional brain networks in children with temporal lobe epilepsy. Epilepsy research, 100(1–2), 168–178. [PubMed: 22418271]

70. Haneef Z, Lenartowicz A, Yeh HJ, Levin HS, Engel J, & Stern JM (2014). Functional connectivity of hippocampal networks in temporal lobe epilepsy. Epilepsia, 55(1), 137–145. [PubMed: 24313597]

71. Engel J, Jr, Thompson PM, Stern JM, Staba RJ, Bragin A, & Mody I (2013). Connectomics and epilepsy. Current opinion in neurology, 26(2), 186. [PubMed: 23406911]

72. Gogtay N, Giedd JN, Lusk L, Hayashi KM, Greenstein D, Vaituzis AC,… & Rapoport JL (2004). Dynamic mapping of human cortical development during childhood through early adulthood. Proceedings of the National Academy of sciences of the United States of America, 101(21), 8174–8179. [PubMed: 15148381]

73. Rausch R, & Walsh GO (1984). Right-hemisphere language dominance in right-handed epileptic patients. Arch Neurol, 41(10), 1077–1080. [PubMed: 6477215]

74. Devinsky O, Perrine K, Llinas R, Luciano DJ, & Dogali M (1993). Anterior temporal language areas in patients with early onset of temporal lobe epilepsy. Annals of neurology, 34(5), 727–732. [PubMed: 8239568]

75. Hamberger MJ (2007). Cortical language mapping in epilepsy: a critical review. Neuropsychology review, 17(4), 477–489. [PubMed: 18004662]

76. Powell HW, Parker GJ, Alexander DC, Symms MR, Boulby PA, Wheeler-Kingshott CA,Duncan JS (2007). Abnormalities of language networks in temporal lobe epilepsy. Neuroimage, 36(1), 209–221. [PubMed: 17400477]

77. Yücel M, Stuart GW, Maruff P, Velakoulis D, Crowe SF, Savage G, & Pantelis C (2001). Hemispheric and gender-related differences in the gross morphology of the anterior cingulate/paracingulate cortex in normal volunteers: an MRI morphometric study. Cerebral Cortex, 11(1), 17–25. [PubMed: 11113032]

Highlights

- In humans and non-human primates, the parahippocampal gyrus (PHg) is subdivided into parahippocampal (PHc) and perirhinal (PRc) cortices which receive input from distinct cortical networks and project distinctly to the entorhinal cortex (ERc) which subsequently projects to the hippocampus.
- With diffusion tensor imaging (DTI), this study visualized and quantified these medial temporal lobe networks.
- While DTI findings in healthy participants mirrored histology findings, in participants with temporal lobe epilepsy the spatial organization of these networks was significantly altered.
- Although the causal relationship between these structural connectivity abnormalities and epilepsy onset is unclear at this time, these findings may relate to the neuroanatomical underpinnings of kindling and may relate to the memory impairments common in temporal lobe epilepsy patients

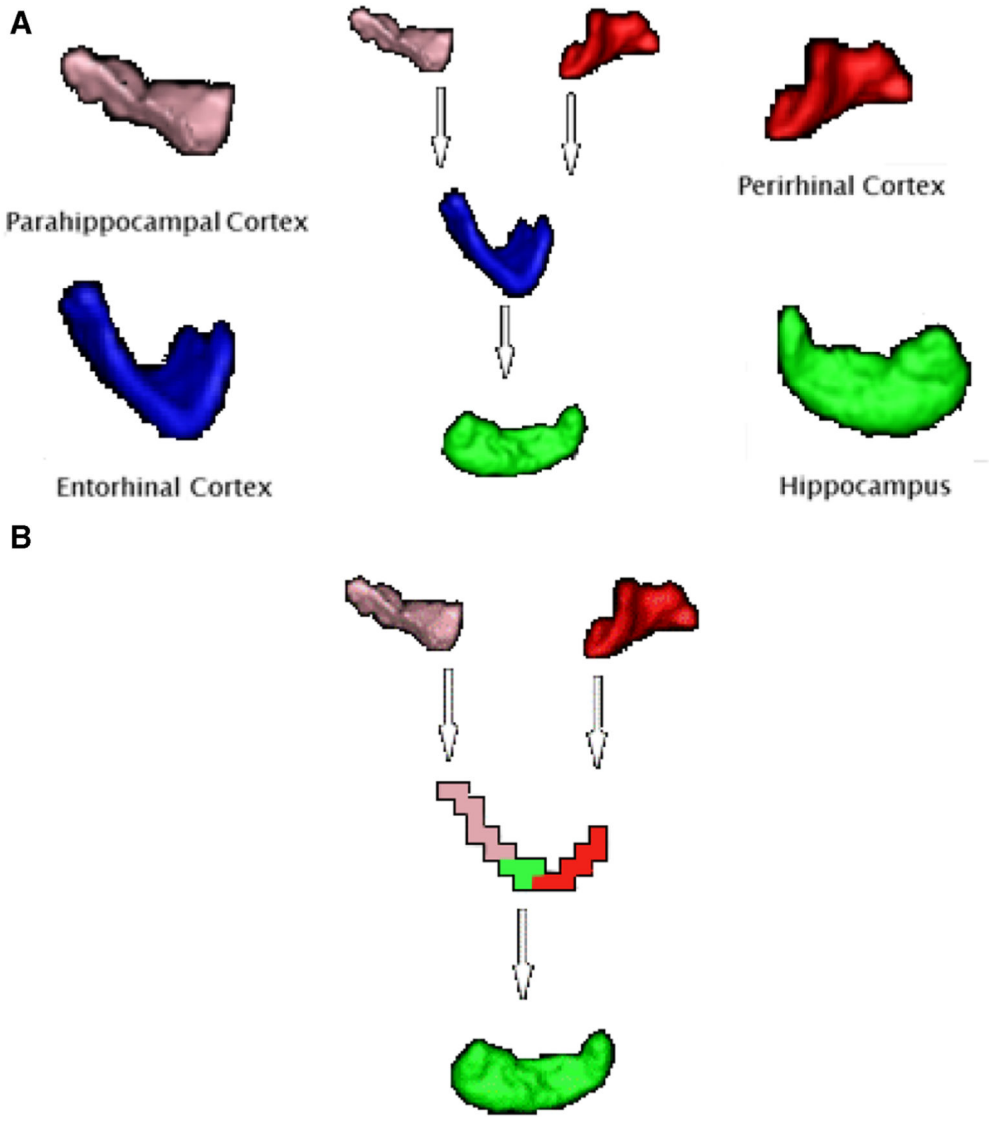

Fig. 1.

Segmented medial temporal lobe structures and resulting connectivity. A). Published protocols for manual segmentation of individual medial temporal lobe regions were used by trained raters to create masks of each participant's PRc, PHc, and ERc. An automated segmentation program, FIRST part of FSL, was used to automatically segment the HC. B).Voxels of the ERc color-coded based on their highest probability of connecting to PHc (pink), HC (green), and PRc (red). Highest probability of connection was defined as the greatest number of streamline samples computed between the seed mask and one of the three target masks. Clearly delineated adjacent temporal lobe connections were easily visualized such that the PRc connects to the medial-ERc, the PHc connects to the lateral-ERc, and the region of the ERc separating PRc and PHc projections is connected to the HC. These results are supported by extant histology literature. (For interpretation of the references to color in this figure legend, the reader is referred to the web version of this article.)

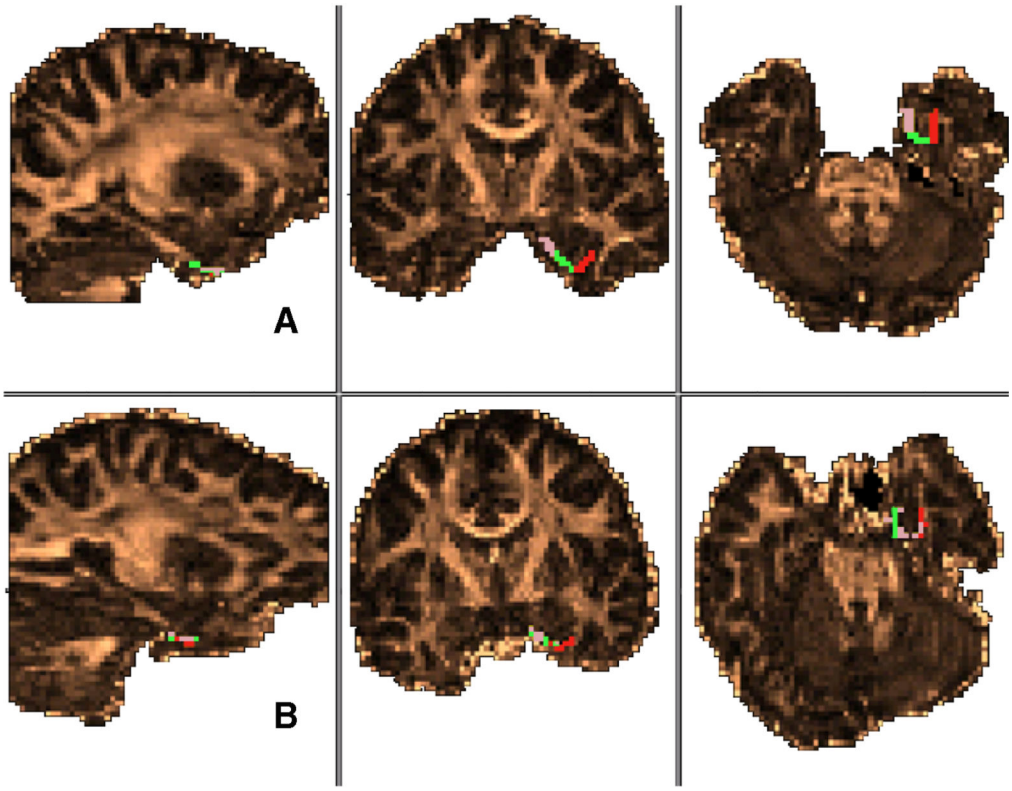

Fig. 2.

Between group comparison of entorhinal cortex connectivity-defined region CDR spatial organization. Spatial organization of the entorhinal cortex in the left hemisphere of a healthy control participant (A) and the epileptogenic hemisphere of a participant with current TLE diagnosis (B). Regions defined by highest probability of connection to parahippocampal cortex (pink), hippocampus (green), and perirhinal cortex (red). (For interpretation of the references to color in this figure legend, the reader is referred to the web version of this article.)

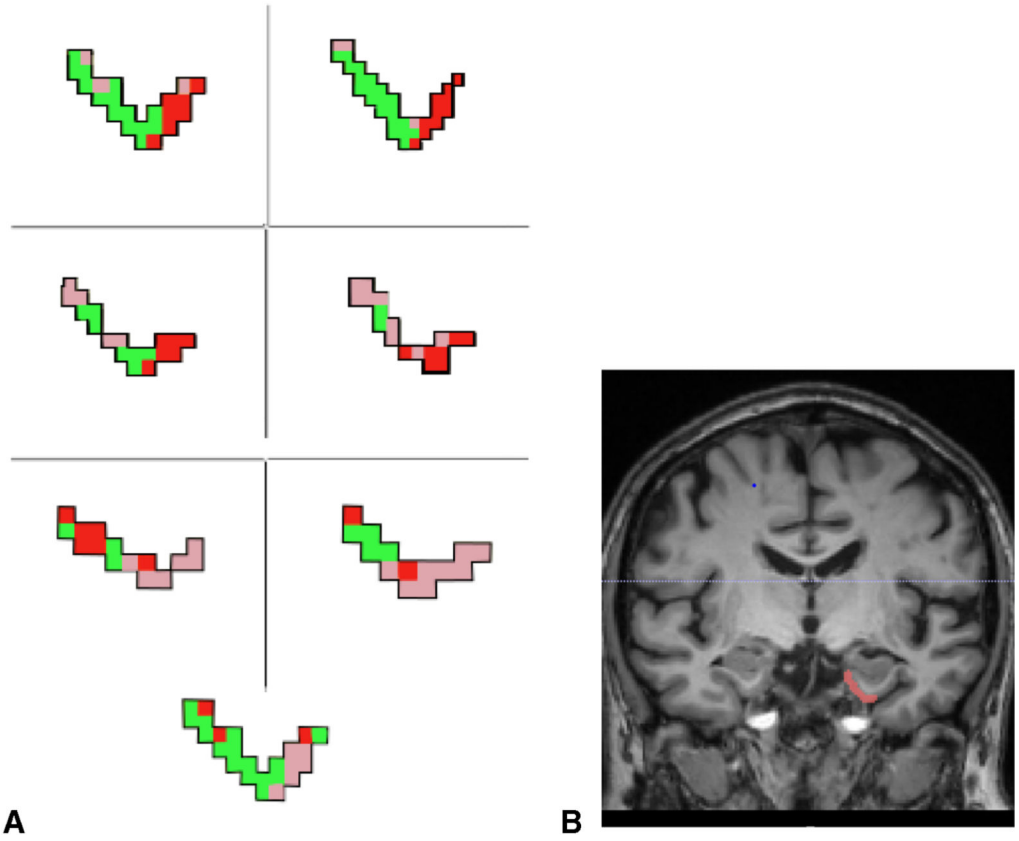

Fig. 3.

Entorhinal cortex connectivity-defined regions in temporal lobe epilepsy. A) Connectivity-based segmentation of the ERc of all patients with TLE demonstrating poor spatial organization of medial temporal lobe connectivity. Again, voxels are color coded based on the target mask with which they share the highest number of streamline samples (e.g., highest connectivity probability). PHc (pink), PRc (red), and HC (green) connectivity-defined regions are not contiguous and do not demonstrate the clearly delineated connectivity pattern seen in health controls. B) Coronal MR slice showing the orientation of the ERc shown in A. (For interpretation of the references to color in this figure legend, the reader is referred to the web version of this article.)

Table 1.

Tractography Participant demographics (N = 14)

	TLE(N=7)		Control (N=7)	
	Mean	**Standard Deviation**	**Mean**	**Standard Deviation**
Age [a]	14.8	3.3	23.9	3.0
Sex	5 Male	2 Female	5 Male	2 Female
Education [b]	9.1	3.9	11.6	1.3
Age at First Seizure [b]	10.0	5.4	-	-
Seizure Duration [b]	4.8	3.5	-	-

Note. All TLE participants were classified by current consensus diagnosis of Complex Partial Temporal Lobe Epilepsy. Current

[a] Years.

[b] N = 14

Author Manuscript

Author Manuscript

Author Manuscript

Table 2.

Within Group Entorhinal Cortex Connectivity-defined Region Clusters

	TLE(N = 7)		Control(N = 7)	
	Mean	**Standard Deviation**	**Mean**	**Standard Deviation**
Epi HC	2.86*	0.69	2.14	0.38
Contra HC	2.00	0.0	2.00	0
Epi PR	2.86*	0.69	1.71	0.49
Contra PR	2.14	0.38	1.71	0.49
Epi PH	2.86	0.38	1.43	0.79
Contra PH	2.71	0.76	1.71	0.49

* $p < 0.05$

Within the TLE group, there were more clusters in the epileptogenic than contralateral hemisphere for the ERc CDR connected to the PRc and HC. In the control group, there were no significant differences in number of clusters between hemispheres.

Table 3.

Within Group Entorhinal Cortex Connectivity-defined Region Proportional Surface Areas

	TLE(N = 7)		Control(N = 7)	
	Mean	**Standard Deviation**	**Mean**	**Standard Deviation**
Epi HC	0.47	0.17	0.54	0.14
Contra HC	0.60 *	0.15	0.59	0.17
Epi PR	0.35 *	0.10	0.33	0.11
Contra PR	0.27	0.11	0.29	0.10
Epi PH	0.18	0.13	0.13	0.06
Contra PH	0.12	0.11	0.11	0.09

* p 0.05

In the epileptogenic hemisphere of the TLE group, the surface area of the PRc CDR was larger and the surface area of the HC was smaller than that of the contralateral hemisphere. In the control group, there were no significant differences in CDR surface area between hemispheres.